

STOCHASTIC MODEL FOR PARTICLE SUSPENSION IN OPEN CHANNELS

By

Kazuo Ashida

Disaster Prevention Research Institute,
Kyoto University, Uji 611, Japan

and

Masaharu Fujita

Disaster Prevention Research Institute,
Kyoto University, Uji 611, Japan

SYNOPSIS

It is important to evaluate non-equilibrium suspended load to analyze armouring process and reservoir sedimentation process in open channels. In this paper, mechanism of particle suspension and pick up rate are investigated, and a stochastic model to calculate suspended load is proposed under both non-equilibrium and equilibrium conditions.

The mechanism of particle suspension is investigated by simultaneous observation of large scale turbulence near the bed and motions of suspended particles. Then, a stochastic model for the motions of suspended particle is formulated from the properties of large scale turbulence and the equation of particle motion. Using this model, the process of vertical dispersion and the streamwise step length of suspended particles are calculated. Furthermore, pick up rate is discussed theoretically and experimentally, by consideration of the shelter effect of gravels in the case of nonuniform sediment, and a method to calculate the concentration distribution of suspended load, which is applicable under both equilibrium and non-equilibrium conditions, is formulated. This model is applied to calculation of non-equilibrium suspended load with armouring process.

INTRODUCTION

There is often need to estimate non-equilibrium suspended load as well as equilibrium suspended load in alluvial channels. For example, in armouring process, the region in which suspended load becomes non-equilibrium may be very long because the grain size distribution of bed materials and hydraulic conditions vary with time and with space. In reservoir sedimentation, suspended load varies in the streamwise direction because the flow is non-uniform. The conventional methods to calculate such suspended load are based on diffusion models. Diffusion models, however, are not always adequate for calculation of non-equilibrium suspended load because it is difficult to give the boundary conditions, the so-called reference level concentration. Other methods are based on stochastic models. They are available for calculation of non-equilibrium suspended load since they are composed of the analysis of the motions of each particle. But these analyses, in which numerical methods are usually used, are generally complicated and have mainly two problems. One concerns the mechanism of particle suspension and the other concerns pick up rate.

The presence of the coherent structure of turbulence has been confirmed by a flow visualization technique and a conditional sampling technique of turbulent velocity. With such researches, recently the relevancy between the coherent structure of turbulence, for example bursting and boiling, and the motions of

suspended particles have been discussed in detail. Jackson, R.G. (9) observed that the sediment concentration was higher in the boil than that in its surrounding during a flood and considered that the kolk eroded fine sand from the bed into the flow. Sumer, B.M. and R. Deigaard (12) made observations of the motions of suspended particles in open channel flows over a smooth bed and a rough bed, and explained the mechanism of particle suspension close to the wall in turbulent flow in terms of the bursting process. But the formulation of model for particle suspension has been incomplete since dynamic forces on a suspended particle has not been satisfactorily examined. On the other side, pick up rate of suspended load has seldom been investigated as the motions of particles near the bed are very complicated, particularly, in the case of non-uniform sediments because of the shelter effect by gravels.

In this paper, particle motions and turbulent flow near a rough bed, which is visualized by dye, are photographed simultaneously, and the relevancy between particle suspension and the bursting process will be explained. Dynamic forces are evaluated from the equation of particle motion and a trajectory. From these results and the characteristics of turbulent flow near the bed, which are investigated by hydrogen bubble method, the motions of particles are formulated by a probabilistic method, and the characteristics of motions of suspended particle are discussed. Moreover, pick up rate is investigated theoretically and experimentally in consideration of the shelter effect, and a method to calculate both equilibrium and non-equilibrium suspended load is proposed. This method is applied to the analysis of the armouring process.

MECHANISM OF PARTICLE SUSPENSION AND TURBULENT FLOW OVER A ROUGH BED

Turbulent Flow over a Rough Bed and its Characteristics

The coherent structure of turbulence, which has usually been observed near a smooth bed, is found to consist of sweep event and ejection event. It is significant to investigate the quantitative and qualitative characteristics of these events in order to discuss the mechanism of particle suspension. As the turbulent structures over a rough bed have been less investigated than those over a smooth bed, in this study the flow patterns and the characteristics of the coherent structure of turbulence over a rough bed were investigated by flow visualization.

The experimental flume was 0.3 m wide and 8 m long and its slope was 0.001. The channel bed was covered by gravel which had a mean diameter of 4.8 mm. Flow discharge was 1.2 l/sec, flow depth was 2.8 cm, shear velocity was 1.5 cm/sec, grain Reynolds number was 72.0 and Reynolds number on mean flow velocity was 4000. The working section was located 5 m downstream from the entrance of the flume. Flow was visualized by hydrogen bubble and dye. In the experiment with hydrogen bubble technique, which was similar to the technique used by Grass, A.J. (6), two dimensional flow patterns through the depth was observed, and these are shown in Photo 1. Hydrogen-bubbles were produced at an interval of 0.02 sec. In the experiment with dye technique, the motions of the fluid mass near the bed were observed. This experiment was also performed for investigating the mechanism of particle suspension. The method used to inject the dye will be mentioned in the next section. A high speed video camera of 200 frames per second was used for photographing.

In Photo 1 (1)~(4) a series of flow patterns visualized by hydrogen-bubbles on a rough bed are shown. The numerical values written in the photos represent the time expressed in 0.001 sec. The ascending process of fluid mass can be seen in (2)~(3) and the descending process of fluid mass can be seen in (1) and (4). This phenomenon is entirely similar to the bursting process, which has been observed over a smooth bed. The event in (2) and (3) corresponds to its ejection event and the event in (1) and (4) corresponds to its sweep event. Fluid mass near the bed rises up suddenly and intermittently, and its vertical scale is usually 20~30 % of the flow depth but sometimes about the flow depth. When the ejection occurs, magnitude of lift force with the motion of the accelerated fluid mass is thought to keep a large positive value near the bed. A particle on the bed must be entrained into the flow by this lift force.

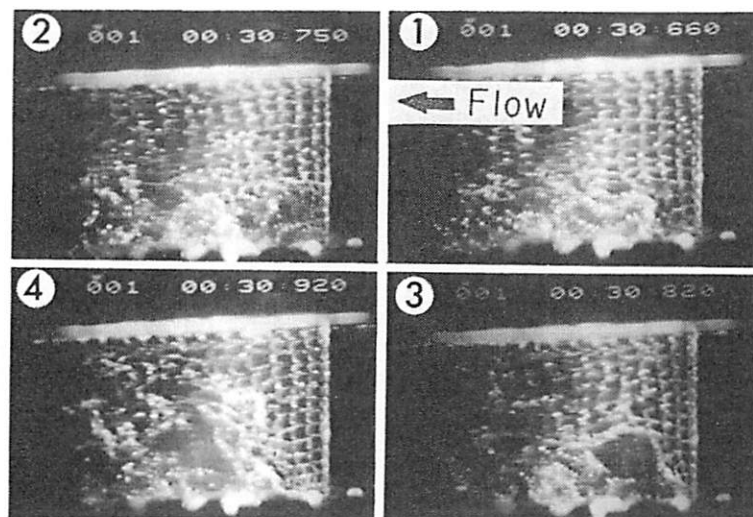


Photo 1 Visualized turbulent flow

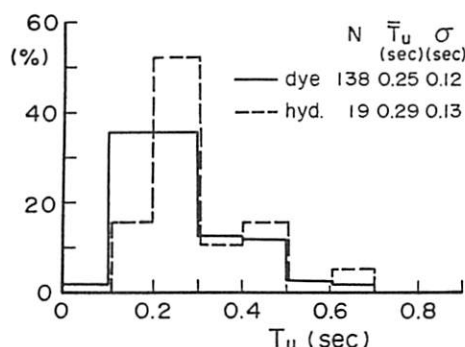


Fig. 1 Period of occurrence of bursting over a rough bed

In Fig. 1 the frequency histogram of the period of occurrence of bursting process is shown. The mean value of the period is 0.27 sec and its nondimensional value $T_u U_{\max}/h$ is 1.7, where T_u = the period of bursting process; U_{\max} = the maximum streamwise flow velocity; and h = the mean flow depth. This value is almost consistent with the period of the bursting over a smooth bed, for example 1.5~3.0 by Nezu, I and H. Nakagawa (10). Thus nondimensional period of occurrence of ejection, $T_u U_{\max}/h$, is found to be independent on the bed conditions.

Lagrangian vertical velocity w_{fe} and the duration time T_{el} of upward flow mass near the bed are the important factors for modeling of motion of suspended particle. A close correlation between T_{el} and w_{fe} is recognized in the experiment. T_{el} and w_{fe} were obtained from the trajectories of hydro-bubbles and the top of the boundary of dyed fluid mass. Fig. 2, expressed in nondimensional forms of T_{el} and w_{fe} , shows that T_{el} has evidently a tendency to increase with w_{fe} near the bed. Although the experimental data are rather scattering, the following relation can be written.

$$\frac{T_{el} u_*}{h} = a \frac{w_{fe}}{u_*} \quad (1)$$

where u_* = shear velocity; and a = a constant.

The validity of Eq.(1) is discussed as follows: In Fig.2 is also shown the relation between the Eulerian vertical velocity w_{fee} and its duration time T_{ee} .

They were measured at mean level of upward flow mass, z_L , which was $0.14h$ in this experiment. The value of T_{e1} and T_{ee} are almost same when w_{fe}/u_* equals w_{fee}/u_* . Since the exact relation between T_{e1} and T_{ee} can not be obtained due to the scattering of the data, it is assumed that T_{e1} is $c_3 T_{ee}$, where c_3 is nearly equal to 1.0. Then the mean value of T_{ee} is expressed as $c_1 \kappa z / \bar{w}_{fee}$ at a level z according to Prandtl's mixing length theory, where κ is the von Kármán's constant and equals about 0.4, and c_1 is a constant. Since both of w_{fe} and w_{fee} is expressed as $c_2 u_*$, a is written as

$$a = \frac{c_1 c_3}{c_2^2} \kappa \frac{z_L}{h} \quad (2)$$

where c_2 is a constant. As the vertical turbulent velocity w_f ($-\infty < w_f < \infty$) follows the Gaussian distribution with mean value zero and standard deviation u_* over a rough bed, c_2 is about 0.67 if the probability density functions of w_{fe} and w_{fee} approximately equal the probability density function of w_f under the condition that $w_f > 0$. As Fig. 2 shows that a is 0.067, c_1 equals about 0.5. Thus, the relation between w_{fe} and T_{e1} is determined only if z_L/h is obtained for a hydraulic condition. The value of z_L/h may not be constant, but it is assumed that z_L/h is about 0.14 from this experiment.

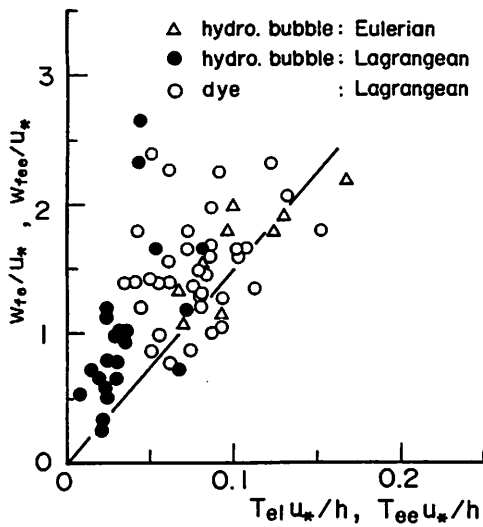


Fig. 2 Relation between turbulent upward flow velocity and its duration

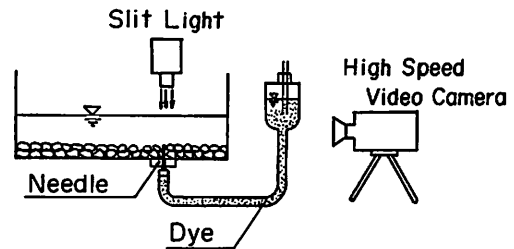


Fig. 3 Experimental apparatus

Mechanism of Particle Suspension over a Rough Bed

The relevancy between the flow near a rough bed and particle suspension was investigated by the following experiment. The experimental flume, hydraulic conditions and bed materials were almost similar to those of the above experiment. Rodamine B solution was used as a tracer and was supplied into the flow near the bed at a constant velocity with the apparatus shown in Fig. 3. The needle was 1 mm in diameter and was inserted through the channel bed. The particles used were polystyrene beads with a diameter of 1.4 mm, a specific weight of 1.05 and a mean fall velocity of 1.88 cm/sec. The flow visualized by dye and the motions of polystyrene beads over a rough bed were simultaneously filmed by a high speed video camera.

The process in which a particle is entrained into the flow from the situation of resting on a rough bed and the process in which it rises up again from the situation of settling in the flow are shown in Photos 2 (a) and 2 (b), respective-

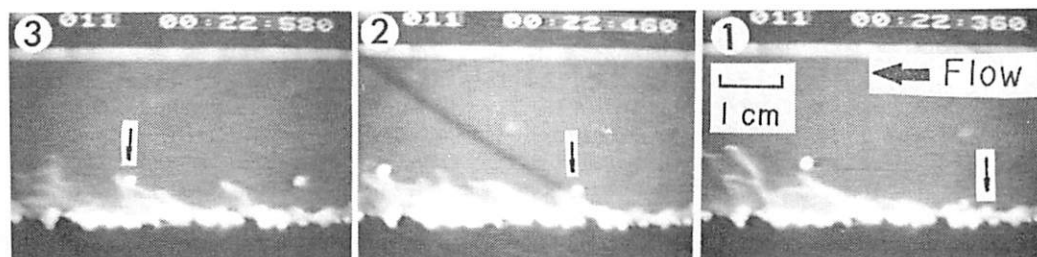


Photo 2 (a) Relation between particle motion and turbulent flow when a particle is entrained from the bed

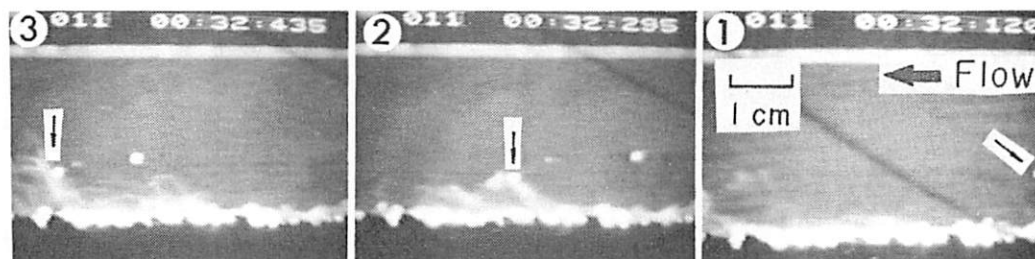


Photo 2 (b) Relation between particle motion and turbulent flow when a particle rises in the process of downward motion

ly. The intermittent occurrence of ejection event is also seen in these photos. Photo 2 (a) shows that a particle is suddenly lifted up together with the ascending fluid mass near the bed. After that, when the particle settles toward the bed, the particle rises up again if the ejection is strong enough to lift it up as shown in Photo 2 (b).

External forces acting on a suspended particle are mainly lift force, drag force and repulsion force by collision with the bed. The motions of the particles transported in saltation are determined only by repulsion force on a bed, and a part of the particles may be turned into suspension by turbulence. Thus, the mechanism of the transformation from saltation to suspension should be investigated. However, the occurrence of such a process was not observed too much over a rough bed in this experiment, and repulsion force should not be included in the mechanism of particle suspension. Lift force and drag force acting on a suspended particle can be recalculated from the observed trajectories of the particles using the equation of particle motion. The forces governing the particle suspension are guessed by this manner. Tchen (7) has represented the equation of vertical particle motion for the Stokes' law regime as

$$\frac{\pi}{6} \sigma d^3 \frac{dw_p}{dt} = F_D + F_L + \frac{1}{2} \frac{\pi}{6} d^3 \rho \left(\frac{dw_f}{dt} - \frac{dw_p}{dt} \right) - G \quad (3)$$

where d = particle diameter; σ = particle density; ρ = fluid density; w_p = vertical velocity of particle; w_f = vertical velocity of fluid; and F_D , F_L , G = drag force, lift force and gravity force in the fluid. F_D , F_L and G are written as

$$F_D = \frac{1}{2} C_D \rho |w_f - w_p| (w_f - w_p) \frac{\pi}{4} d^2 \quad (4)$$

$$F_L = \frac{\pi}{6} d^3 \rho \frac{dw_f}{dt} \quad (5)$$

$$G = \frac{\pi}{6} (\sigma - \rho) g d^3 \quad (6)$$

where C_D = the coefficient of drag force and $C_D = 24 \nu / |w_f - w_p| d$.

The variation of F_D and F_L along a trajectory of suspension can be calculated from Eq.(3)~(6). In Fig. 4 is shown an example of a trajectory by experiment and the variation of F_L with time. F_L is smoothed by moving average method from $F_L = (F_{Li-1} + F_{Li} + F_{Li+1})/3$, where $F_{Li} = F_L$ calculated from Eq.(3)~(6) after 0.01 sec from the entrainment. The errors in the calculation of F_L may not be small because of the inaccuracy of the trajectory, but Fig. 4 indicates that F_L is positive and large for a short time when a particle is entrained, and suddenly decreases to about zero. The frequency histogram of the time mean value of this positive and large lift force, F_{L0} , is shown in Fig. 5. The broken line expresses the Gaussian distribution which has a mean value of zero dyne and a standard deviation of 0.15 dyne under the condition that $F_{L0} > G$. The probability density function of F_{L0} is thought approximately to follow the Gaussian distribution. In Fig. 6 frequency histogram of the thickness Δ within which lift force keeps positive from the bed is shown. In this experiment Δ is found to be about $0.5d$. As experimental condition is only a case, it is uncertain to apply this relation generally, but it is assumed that Δ is $0.5d$ from this experimental results. As the mean lift force was -0.0069 dyne for $z > \Delta$, it seems that F_{L0} decreases to zero within $0.5d$ from the bed. In Fig. 7 the variation of drag force F_D with time and the trajectory in the case that F_L is taken to be zero for $z > \Delta$ is shown. The particle moves upward or downward being effected by the drag force of large scale turbulence.

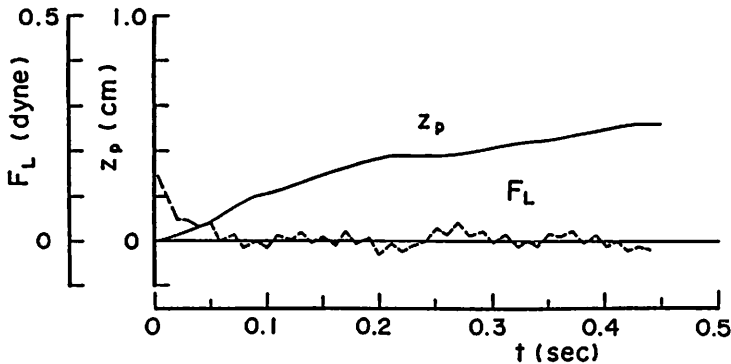


Fig. 4 Variation of lift force along a trajectory of suspended particle

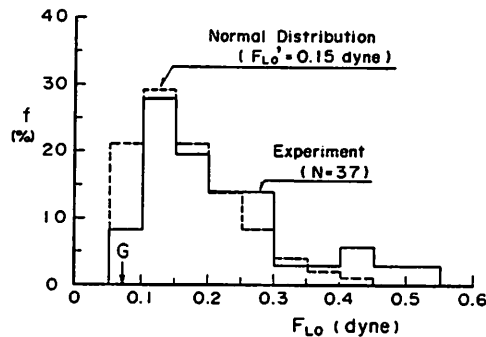


Fig. 5 Frequency histogram of lift force near the bed by ejection

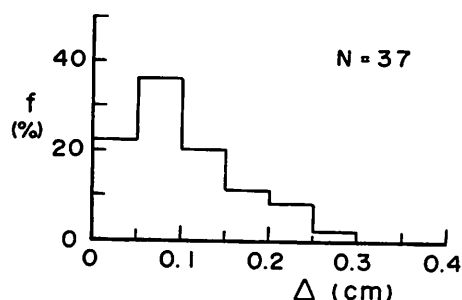


Fig. 6 Frequency histogram of depth within which lift force near the bed is positive when ejection occurs

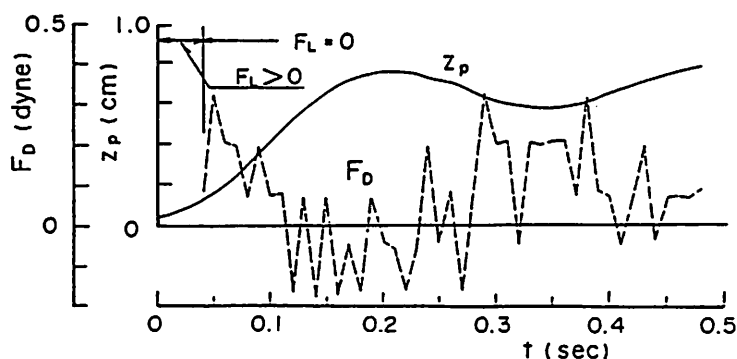


Fig. 7 Variation of drag force along a trajectory of suspended particle

From these results the mechanism of particle suspension can be considered in terms of bursting or macro-turbulence as follows: A particle on a rough bed is entrained by lift force F_{L0} due to the accelerated upward flow near the bed which is produced when an ejection event occurs. Though F_{L0} decreases to zero in short time t_{*} , if the duration of the upward flow, T_{e1} , is larger than t_{*} , drag force F_D acts on a particle during $T_{e1} - t_{*}$. After that, the particle is transported in suspension by the drag force due to upward or downward turbulent flow.

A STOCHASTIC MODEL OF PARTICLE SUSPENSION

A Model of the Motions of a Suspended Particle over a Rough Bed

A model of the vertical and streamwise motions of a particle entrained from a rough bed is thought under the following hypotheses. (see Fig. 8)

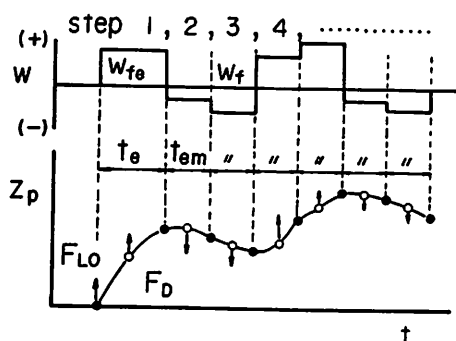


Fig. 8 A model for mechanism of particle suspension

(i) Two dimensional uniform turbulent flow is considered.

(ii) The vertical motions are divided into step 1,2,..... by Lagrangean duration of turbulent flow velocity. A particle is drifted by the following forces in each step. In step 1 (the process of entrainment from the bed), lift force F_{LO} acts on a particle on the bed during its duration t_* , and after that drag force F_D by upward flow acts on it during $t_e - t_*$, where t_e is the duration of upward flow near the bed. In step 2,3,4,..... (the process of suspension), the particle rises or settles by the effect of drag force F_D due to upward or downward turbulent flow velocity w_f , and eventually returns to the bed. Time step t_{em} is constant and assumed to be the mean duration of w_f at the mean elevation of suspended particle.

(iii) Streamwise velocity of a suspended particle, u_p , is assumed to equal the flow velocity at its time mean elevation after entrainment from a bed.

The vertical particle motions will be formulated by Eq.(3). If F_{LO} finishes acting on a particle at $t = 0$, lift force F_L can be negligible after $t = 0$. Hence Eq.(3) in non-dimensional form is described

$$\frac{d\hat{w}_p}{d\hat{t}} = \frac{6}{\pi} \frac{2}{2s+3} \hat{F}_D - \frac{2s}{2s+3} \quad (7)$$

where $\hat{w}_p = w_p/\sqrt{gd}$; $\hat{t} = t/\sqrt{d/g}$; $s = \sigma/\rho - 1$; and $\hat{F}_D = F_D/\rho g d^3$. In the following description $\hat{\cdot}$ signifies non-dimensional value by ρ , d and g .

Considering the regime which Stokes' law can not apply to, according to Rubey's theory, the coefficient of drag force is expressed as

$$C_D = 2 + \frac{24\hat{v}}{|\hat{w}_f - \hat{w}_p|} \quad (8)$$

where $\hat{w}_f = w_f/\sqrt{gd}$; $\hat{v} = \nu/\sqrt{d^3g}$; and ν = kinematic viscosity. Eqs.(4) and (8) can be applied for the conditions that relative streamwise velocity between particle and fluid, $u_p - u_f$, is small. As u_p is nearly equal to u_f , it may safely be said that the errors in calculation of F_D are neglected.

From Eqs.(4) and (8), Eq.(7) is reduced to

$$\frac{d\hat{w}_p}{d\hat{t}} = A|\hat{w}_f - \hat{w}_p|(\hat{w}_f - \hat{w}_p) + B(\hat{w}_f - \hat{w}_p) + C \quad (9)$$

$$\text{where } A = \frac{3}{2s+3}, \quad B = \frac{36}{2s+3} \hat{v}, \quad C = -\frac{2s}{2s+3}$$

Eq.(9) can be solved under the initial conditions of each step on the vertical velocity and elevation of particle. The solutions on \hat{w}_p and non-dimensional particle elevation \hat{z}_p ($= z_p/d$) are formally expressed as

$$\hat{w}_p(\hat{t}) = F_1(\hat{w}_{p0}, \hat{w}_{fe}, \hat{t}) \quad (10-a)$$

(step 1)

$$\hat{z}_p(\hat{t}) = G_1(\hat{w}_{p0}, \hat{z}_{p0}, \hat{w}_{fe}, \hat{t}) \quad (10-b)$$

$$\hat{w}_p(\hat{t}) = F_i(\hat{w}_{pi-1}, \hat{w}_f, \hat{t}) \quad (11-a)$$

(step i, i = 2,3,.....)

$$\hat{z}_p(\hat{t}) = G_i(\hat{w}_{pi-1}, \hat{z}_{pi-1}, \hat{w}_f, \hat{t}) \quad (11-b)$$

where $\hat{w}_{fe} = w_{fe}/\sqrt{gd}$; \hat{w}_{pi-1} = initial conditions on \hat{w}_p in step i; \hat{z}_{pi-1} = initial conditions on \hat{z}_p in step i; \hat{t} = past time in each step; w_{fe} = the vertical turbulent velocity acting on a particle in step 1; and F_i and G_i = the function of

each parameter in bracket.

The initial conditions, the vertical turbulent velocity and its duration are given in each step as follows:

In Step 1, the initial particle elevation z_{p0} equals the thickness Δ within which F_{L0} acts on a particle. As Fig. 6 indicates that Δ is about $0.5d$,

$$\hat{t} = 0 ; \quad \hat{z}_{p0} = 0.5 \quad (12)$$

where $\hat{z}_{p0} = z_{p0}/d$.

The initial vertical particle velocity \hat{w}_{p0} is obtained from the equation of impulse as

$$(\hat{F}_{L0} - \hat{G}) \hat{t}_* = (\pi/6)(s+1) \hat{w}_{p0} \quad (13)$$

where $\hat{G} = G/\rho g d^3$; $\hat{F}_{L0} = F_{L0}/\rho g d^3$; $\hat{t}_* = t_*/\sqrt{d/g}$; $\hat{w}_{p0} = w_{p0}/\sqrt{gd}$; t_* = the duration of F_{L0} ; and t_* is assumed to be $\Delta/0.5w_{p0}$. So \hat{w}_{p0} is obtained as

$$\hat{w}_{p0} = \sqrt{\frac{6}{\pi} \frac{1}{s+1} (\hat{F}_{L0} - \hat{G})} \quad (14)$$

The probability density function (p.d.f.) of F_{L0} is supposed to be expressed by the Gaussian distribution with a mean value of zero. Its standard deviation \hat{F}_{L0}' may be defined as $cpw_f'^2 d^2$, where w_f' is vertical turbulent intensity and c is the coefficient of lift force. Although w_f' is almost equal to u_* near a rough bed as seen experimentally, it decreases to ku_* among the gravels by the shelter effect, where k is the coefficient of shelter effect. So \hat{F}_{L0}' becomes

$$\hat{F}_{L0}' = ck^2 \hat{u}_*^2 \quad (15)$$

where $\hat{u}_* = u_*/\sqrt{gd}$. Hence the p.d.f. of \hat{F}_{L0} is expressed as

$$\hat{f}_{F_{L0}}(\hat{F}_{L0}) = \frac{1}{\sqrt{2\pi} ck^2 \hat{u}_*^2} \exp \left\{ -\frac{1}{2} \left(\frac{\hat{F}_{L0}}{ck^2 \hat{u}_*^2} \right)^2 \right\} \quad (16)$$

From Eqs.(14) and (16), the p.d.f. of \hat{w}_{p0} is expressed as

$$\begin{aligned} \hat{f}_{w_{p0}}(\hat{w}_{p0}) &= \frac{\sqrt{2\pi} (s+1) \hat{w}_{p0}}{6 \hat{F}_{L0}'} \exp \left[-\frac{1}{2} \left\{ \frac{(\pi/6)(s+1) \hat{w}_{p0} + \hat{G}}{\hat{F}_{L0}'} \right\}^2 \right] \\ &\quad / \int_{\hat{G}}^{\infty} \hat{f}_{F_{L0}}(\hat{F}_{L0}) d\hat{F}_{L0} \end{aligned} \quad (17)$$

Vertical flow velocity w_{fe} should be related to F_{L0} , but it is very difficult to derive the relation between F_{L0} and w_{fe} physically. So it is assumed that the probability of occurrence of lift force and vertical flow velocity in excess of \hat{F}_{L0} and \hat{w}_{fe} , which occur with an upward flow mass near a bed, are the same. If \hat{w}_{fe} follows the Gaussian distribution with a mean value of zero and a standard deviation of \hat{u}_* under the condition that $\hat{w}_{fe} > 0$, the relation between them is expressed as

$$\hat{w}_{fe} = \hat{F}_{L0}/(ck^2 \hat{u}_*) \quad (18)$$

The duration of upward flow, t_e , is equal to T_{e1} and t_* is expressed as

Δ/w_{p0} . So the duration of \hat{w}_{fe} , $\hat{t}_e - \hat{t}_*$, is written as the following equation from Eqs.(1) and (14).

$$\hat{t}_e - \hat{t}_* = a \frac{\hat{w}_{fe} \hat{h}}{\hat{u}_*^2} - \frac{\sqrt{\pi(s+1)}}{\sqrt{6(\hat{f}_{L0} - \hat{G})}} \quad (19)$$

where $\hat{h} = h/d$; and a is assumed to be taken to be 0.067.

In step 2,3,..., the p.d.f. of \hat{z}_p at the end of an step and the mean value of \hat{w}_p at the end of an step are given as initial conditions on \hat{z}_p and \hat{w}_p in the next step. \hat{w}_f is given as a random value according to the Gaussian distribution with a mean value of zero and a standard deviation of \hat{u}_* as

$$\hat{f}_{wf}(\hat{w}_f) = \frac{1}{\sqrt{2\pi} \hat{u}_*} \exp \left\{ -\frac{1}{2} \left(\frac{\hat{w}_f}{\hat{u}_*} \right)^2 \right\} \quad (20)$$

Its duration \hat{t}_{em} , which is the mean duration of turbulent flow at the mean elevation of suspended particles, is assumed to be described by the same way to derive Eqs.(1) and (2) as

$$\hat{t}_{em} = \frac{c_1 c_3}{c_2} \frac{\hat{h}}{\hat{u}_*} \eta_s \quad (21)$$

where $\eta_s = z_{ps}/h$; and z_{ps} = the mean elevation of a suspended particle.

Next, the mean streamwise particle velocity from $t = 0$ to $t = T$, $u_p(T)$, is assumed to equal the mean streamwise flow velocity at the time average particle elevation between $t = 0$ and $t = T$. According to the logarithmic law $\hat{u}_p(\hat{T})$ is expressed as

$$\hat{u}_p(\hat{T})/\hat{u}_* = 8.5 + 5.75 \log(\hat{z}_{pm}/\hat{k}_s) \quad (22)$$

where $\hat{u}_p(\hat{T}) = u_p(T)/\sqrt{gd}$; $\hat{k}_s = k_s/d$; $\hat{z}_{pm} = z_{pm}/h$; k_s = the equivalent sand roughness; and z_{pm} = the time average particle elevation between $t = 0$ and $t = T$.

It is considered that z_{pm} is different from the mean particle elevation at $t = T$ because the particle settles at the fall velocity w_0 on the average. If all the particles which are being suspended at $\hat{t} = \hat{T}$ have settled from $\hat{z}_{p0} = \min(\hat{h}, \hat{z}_{pmT} + \hat{w}_0 \hat{T})$ to \hat{z}_{pmT} at $\hat{t} = \hat{T}$, \hat{z}_{pm} is written as

$$\hat{z}_{pm} = (\hat{z}_{p0} + \hat{z}_{pmT})/2 \quad (23)$$

where z_{pmT} = the mean particle elevation at $t = T$; and w_0 = the fall velocity of particle.

\hat{z}_{pmT} is calculated from the p.d.f. of \hat{z}_p at $\hat{t} = \hat{T}$, $f(\hat{z}_p, \hat{T})$, which is obtained in the next section, as

$$\hat{z}_{pmT} = \int_0^{\hat{h}} \hat{z}_p f(\hat{z}_p, \hat{T}) d\hat{z}_p / \int_0^{\hat{h}} f(\hat{z}_p, \hat{T}) d\hat{z}_p \quad (24)$$

Probabilistic Analysis of Particle Motion

Characteristics of particle motions will be analyzed in detail by a probabilistic method. First, the p.d.f. of elevation where the particle entrained at $\hat{t} = 0$ stays at $\hat{t} = \hat{T}$, $f(\hat{z}_p, \hat{T})$, is led by the following manner. The p.d.f. of elevation where a particle stays after \hat{t} from the terminal time of step i is

expressed from Eqs.(11-b) and (20) as

$$\eta(\hat{z}_p, \hat{t} | \hat{w}_{pi}, \hat{z}_{pi}) = \hat{f}_{wf}(\hat{w}_f) d\hat{w}_f / dG_{i+1}(\hat{w}_{pi}, \hat{z}_{pi}, \hat{w}_f, \hat{t}) \quad (25)$$

where \hat{z}_{pi} = elevation of particle at the end of step i ; and w_{pi} = vertical velocity of particle at the end of step i .

Under the conditions that a particle rises up to the elevation of \hat{z}_{p1} at the end of step 1, the p.d.f. of \hat{z}_p at the end of step i , $g_i(\hat{z}_p | \hat{z}_{p1})$, is obtained from

$$g_{i+1}(\hat{z}_{pi+1} | \hat{z}_{p1}) = \int_0^{\hat{h}} g_i(\hat{z}_{pi} | \hat{z}_{p1}) \eta(\hat{z}_{pi+1}, \hat{t}_{em} | \hat{w}_{pi}, \hat{z}_{pi}) d\hat{z}_{pi} \quad (i = 2, 3, \dots) \quad (26-a)$$

$$g_2(\hat{z}_{p2} | \hat{z}_{p1}) = \eta(\hat{z}_{p2}, \hat{t}_{em} | \hat{w}_{p1}, \hat{z}_{p1}) \quad (26-b)$$

From Eqs. (11-a) and (20), \hat{w}_{pi} can be written as

$$\hat{w}_{pi} = \int_{-\infty}^{\infty} \hat{w}_p f_{wf}(\hat{w}_f) \frac{d\hat{w}_f}{dF_i(\hat{w}_{pi-1}, \hat{w}_f, \hat{t}_{em})} d\hat{w}_p \quad (27)$$

Now, if the particle moves in step n at $\hat{t} = \hat{T}$, the p.d.f. of particle elevation at $\hat{t} = \hat{T}$ under the condition of $\hat{z}_p = \hat{z}_{p1}$ at the end of step 1 can be written as

$$h(\hat{z}_p, \hat{T} | \hat{z}_{p1}) = \int_0^{\hat{h}} g_{n-1}(\hat{z}_{pn-1} | \hat{z}_{p1}) \eta(\hat{z}_p, \delta\hat{t} | \hat{w}_{pn-1}, \hat{z}_{pn-1}) d\hat{z}_{pn-1} \quad (n > 1) \quad (28-a)$$

$$h(\hat{z}_p, \hat{T} | \hat{z}_{p1}) = \delta(\hat{z} - \hat{z}_p(\hat{T})) \quad (n = 1) \quad (28-b)$$

where δ = Dirac delta function; δt is the past time to $t = T$ from the terminal time of step $i-1$; and $\hat{z}_p(\hat{T})$ = the function G_i corresponding to $\hat{z}_p(\hat{t}_e) = \hat{z}_{p1}$. The p.d.f. of \hat{z}_{p1} is calculated from Eq.(10-b) as

$$\hat{\xi}(\hat{z}_{p1}) = \hat{f}_{wfe}(\hat{w}_{fe}) d\hat{w}_{fe} / dG_1(\hat{w}_{p0}, \hat{z}_{p0}, \hat{w}_{fe}, \hat{t}_e) \quad (29)$$

where $\hat{f}_{wfe}(\hat{w}_{fe})$ = the p.d.f. of \hat{w}_{fe} and is similar to Eq.(20).

From these equations, $f(\hat{z}_p, \hat{T})$ is calculated by the numerical method from

$$f(\hat{z}_p, \hat{T}) = \int_0^{\hat{h}} h(\hat{z}_p, \hat{T} | \hat{z}_{p1}) \hat{\xi}(\hat{z}_{p1}) d\hat{z}_{p1} \quad (30)$$

Using Eq.(30), the p.d.f. of non-dimensional duration of particle suspension, $\hat{f}_{ts}(\hat{t}_s)$, is expressed as

$$\hat{f}_{ts}(\hat{t}_s) = \int_0^{\hat{h}} \{df(\hat{z}_p, \hat{t}_s) / d\hat{t}_s\} d\hat{z}_p \quad (31)$$

The non-dimensional step length of suspended particle, $\hat{X}_p (= X_p/d)$ becomes $\hat{u}_p(\hat{t}_s) \hat{t}_s$ and its p.d.f. is described as

$$\hat{f}_{X_p}(\hat{X}_p) = \hat{f}_{t_s}(\hat{t}_s) \cdot d\hat{t}_s/d\hat{X}_p \quad (32)$$

Coefficient of Lift Force and the Shelter Effect

The coefficient of the shelter effect, k , and the coefficient of lift force, c , must be given to determine the p.d.f. of F_{LO} . It is thought that k and c vary with grain size Reynolds number $R_* = u_* d_m/\nu$ and non-dimensional particle elevation Δ_s/d_r , respectively, where d_m = the mean diameter of particles on a bed; d_r = the representative bed roughness; and Δ_s = the distance between particle surface and the top of the representative roughness as shown in Fig. 21. It is very difficult to derive the relation between c and R_* , and the relation between k and Δ_s/d_r physically. So these relations may be presumed from experimental results on the threshold conditions of particle suspension.

A particle will be entrained into the flow from a bed if $F_{LO} > G$. When $\tau_{*s} = (\pi/6)/(\alpha k^2)$, the probability of the entrainment of bed particle is equal to the probability of $F_{LO} > \alpha F_{LO}'$, where τ_{*s} is the critical non-dimensional tractive force concerning suspension. If α is taken to be 3.0 for experimental criterion of suspension, c can be obtained from τ_{*s} by experiment in the case of uniform sediment, namely, $k = 1$. From authors' results concerning τ_{*s} (4), the relation between c and R_* is interpolated as Fig. 9. Einstein's results (5) are also shown in this figure. Then, using Fig. 9 and experimental relations between τ_{*s} and Δ_s/d_r obtained in ref.(4) and the experiment mentioned in the next section, the relation between k and Δ_s/d_r become as shown in Fig. 10

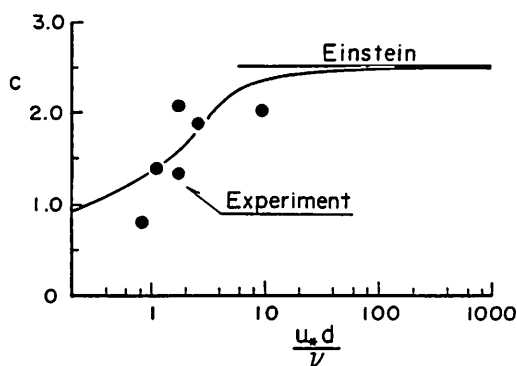


Fig. 9 Coefficient of lift force

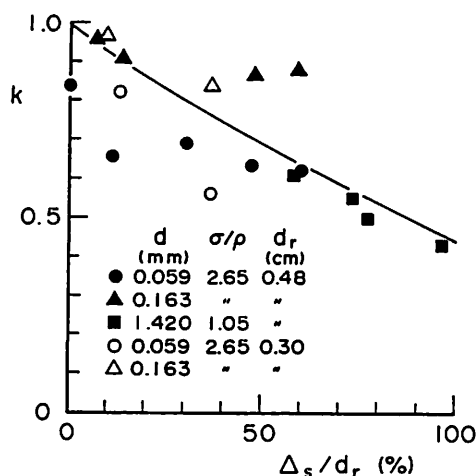


Fig. 10 Coefficient of shelter effect

Comparison Between Theoretical Results and Experimental Results on the Characteristics of Suspended Particles

In Fig. 11 the theoretical results of $f(\hat{z}_p, \hat{T})$ and $\hat{f}_{t_s}(\hat{t}_s)$ under the conditions of $\sigma/\rho = 1.05$, $\tau_* = 0.34$, $\hat{h} = 19.7$, $\hat{U} = 1.27$, $ck^2 = 2.0$ and $\eta_s = 0.17$ are shown. In this figure the results obtained by video analysis of experiment with polystyrene beads are also plotted. This figure shows that the present model sufficiently accounts for the vertical dispersion of particles. In Fig. 12 experimental and theoretical results of excess probability of step length is shown. This figure shows that the streamwise dispersion of particles can also be estimated from the present model. These results show that this model is satis-

factorily applicable to the simulation of the motions of suspended particles.

X_p for excess probability of zero corresponds to the distance X_e in which concentration of suspended load increases to equilibrium value from zero. This is an important parameter for analysis of non-equilibrium suspended load. If this value is small, suspended load reaches equilibrium in a short distance, and it is enough to evaluate suspended load under the equilibrium condition. But if not, there is need to evaluate suspended load under the non-equilibrium condition in order to predict sediment load, the variation of bed elevation and grain size

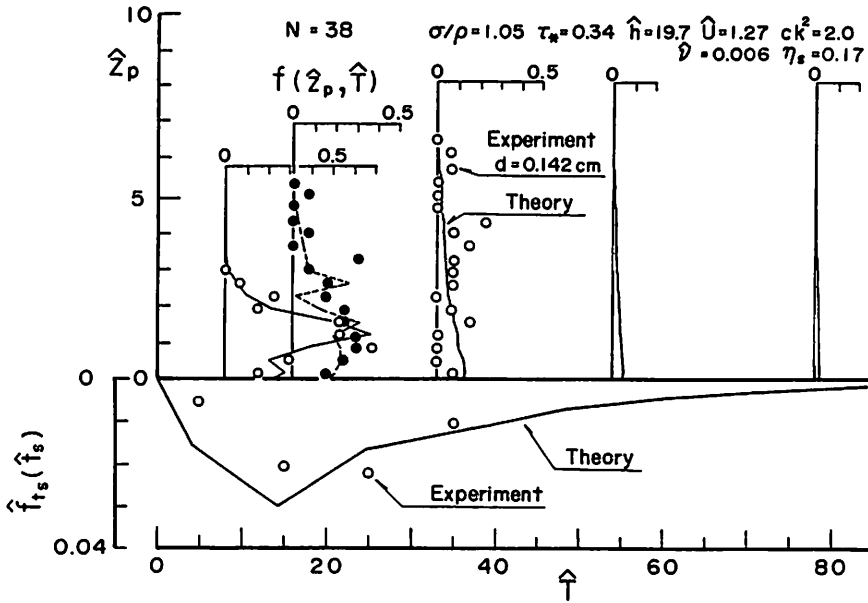


Fig. 11 The process of vertical dispersion of suspended particle and the p.d.f. of duration of suspension

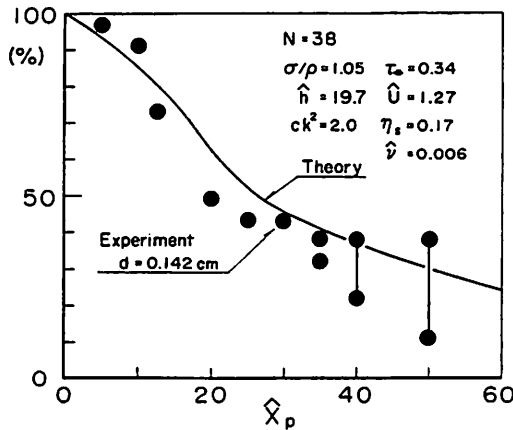


Fig. 12 Excess probability of step length of suspended particle

distribution of bed materials. Figure. 13 shows that variation of $\hat{X}_e (= X_e/d)$ and the non-dimensional mean step length $\hat{X}_{Lm} (= X_{Lm}/d)$ with τ_* under the conditions that $\sigma/\rho = 2.65$, $I = 0.002$, $k_s/d = 2.0$, $ck^2 = 2.0$, $\eta_s = 0.5$ and $\tau_* = 0.32$. When τ_* becomes more than 10, \hat{X}_e might be more than 10^6 . Thus, \hat{X}_e is generally large, and the calculation of non-equilibrium suspended load might be required in the alluvial channel.

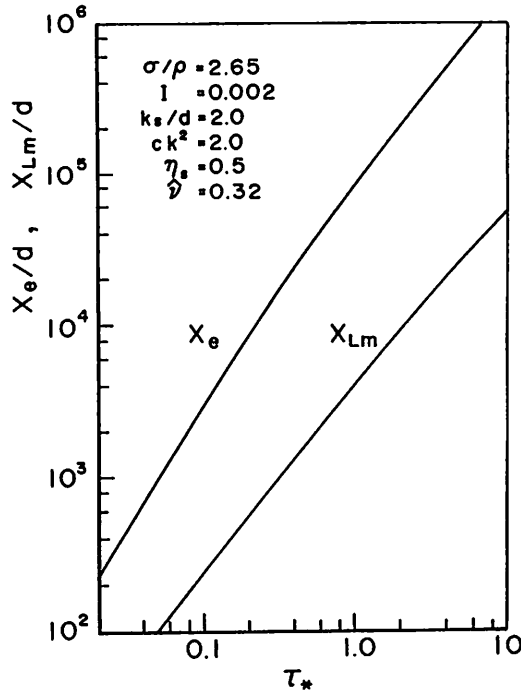


Fig. 13 Relation between maximum step length or mean step length of suspended particle and non-dimensional tractive force

A METHOD TO CALCULATE SUSPENDED LOAD

Pick up Rate of Suspended particles

A particle on a bed is thought to be entrained by lift force and be transformed into suspension in a characteristic time, the so called exchange time. In the case of non-uniform sediments, a particle is remarkably influenced by shelter effect due to gravels. Therefore, it is necessary to evaluate the exchange time and the shelter effect accurately in order to calculate pick up rate. The present theory on calculation of pick up rate is investigated here by consideration of the shelter effect and based on the exchange time.

A particle on a bed is assumed to be entrained and to become a suspended particle in exchange time t_c . Pick up rate q_{su} of the particle entrained per unit time from unit area is expressed

$$q_{su} = k_1 \frac{\pi}{6} \sigma d^3 N_B \int_0^{\infty} (1/t_c) f_{t_c}(t_c) dt_c \quad (33)$$

where k_1 = the rate of the particles able to be picked up to all the particles on the bed surface; N_B = the number of particles per unit area; and $f_{t_c}(t_c)$ is the p.d.f. of t_c .

If t_c is proportional to t_* , t_c becomes

$$t_c = k_2 (d/w_{p0}) \quad (34)$$

where k_2 = a constant.

N_B is written as

$$N_B = p_f \frac{1}{(\pi/4) d^2} \quad (35)$$

where p_f = the rate of particle with diameter d within the materials on the bed surface.

Using Eqs.(14), (16), (33), (34) and (35), q_{su} is written

$$q_{su} = K p_f \frac{2}{3} \sqrt{6\sigma/\pi} \int_G^{\infty} \frac{1}{\sqrt{2\pi F_{L0}'}} \exp\left(-\frac{1}{2} \left(\frac{F_{L0}}{F_{L0}'}\right)^2\right) dF_{L0} \quad (36)$$

where $K = k_1/k_2$.

Then with $\eta = F_{L0}/F_{L0}'$ and $G = C_D \rho w_0^2 (\pi/8) d^2$, Eq.(36) is expressed in non-dimensional form as

$$\hat{q}_{su} = \frac{2}{3} K p_f \sqrt{6(s+1)/\pi} \int_{\eta_0}^{\infty} \frac{1}{\sqrt{2\pi}} \exp\left(-\frac{1}{2} \eta^2\right) d\eta \quad (37)$$

where $C_{D0} = 2+24\nu/(w_0 d)$, $\eta_0 = (\pi/8) C_{D0} \xi_0^2 / (ck^2)$, and $\xi_0 = w_0/u_*$.

The validity of Eq.(37) was investigated by the following experiment. The experimental flume was 8 m long and 30 cm wide. The sand feeder was set up at the 5 m downstream section from the entrance to supply the particles through the gravel bed as shown in Fig. 14. The grain diameter of bed roughness was 4.8 mm. The used particles were polystyrene beads with a diameter of 1.42 mm and a specific gravity of 1.05. The particle motions were photographed by a high speed video camera from the side when the elevation of the bed surface of particles among the gravels was steady under the constant discharge and the constant sediment discharge. Similar experiments were done under various discharge and sediment discharge. Pick up rate was obtained for the parameters of w_0/u_* and Δ_s/d_r by video analysis.

The experimental data on pick up rate are shown in Fig. 15. The value of ck^2 was obtained by Figs. 9 and 10. Pick up rate varies considerably with the shelter effect as shown in this figure. As the shelter effect is evaluated appropriately in this theory, the theoretical curves agree with the experimental results when constant K is taken to be 0.035, which can be physically explained as follows: It is considered that k_1 is related to condition of contact with the neighbour particles. That is to say, k_1 is assumed to equal the probability in which all tangents of a particle with the neighbour particles are opened upward as shown in Fig. 16. Assuming that the number of neighbour particles is n , the probability, therefore, becomes $(1/2)^n$. The relation between the porosity λ and the number of particles contacting a particle in the random packing, n_0 , is shown in Fig. 17 (ref.(11)). If n/n_0 represents the probability in which the center of a contacting particle is located between the upper side elevation and lower side elevation of a contacted particle, n/n_0 becomes 0.5, and the relation between λ and n become as shown in Fig. 17. From this figure K becomes 0.044 for $\lambda = 0.4$, which is similar to the experimental value, as k_2 is assumed to be about 1.

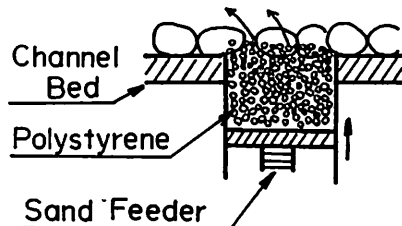


Fig. 14 Sand feeder

In Fig. 15 theoretical curves by Ashida and Michiue (2) and Itakura and Kishi (8) in the case of uniform sediment are also shown. Though the results for uniform sediment by Eq.(37), which is expressed by the line of $ck^2 = 2.5$ when $R_* > 50$, are somewhat larger than their results, the tendency is almost similar. Thus, the present theory will be applicable to calculation of pick up rate for both uniform and nonuniform sediment.

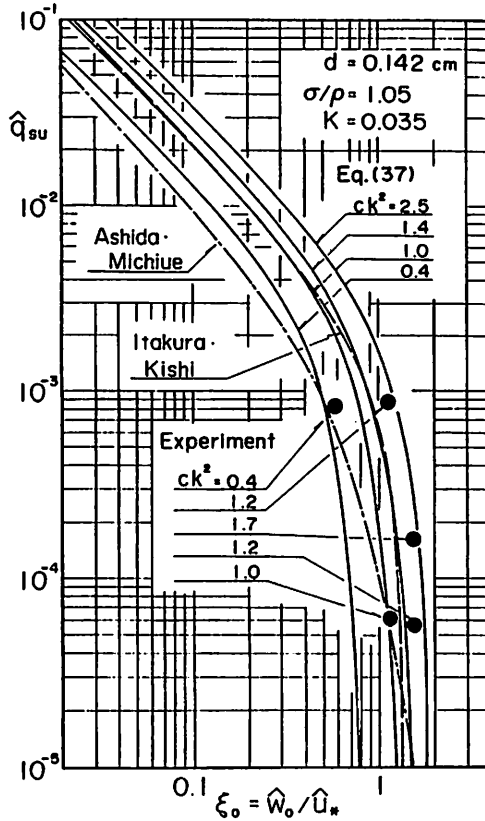


Fig. 15 Comparison between theoretical results and experimental ones concerning pick up rate

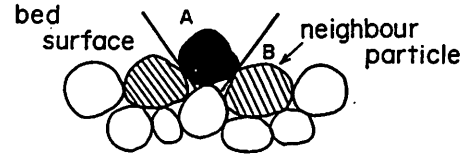


Fig. 16 Situation of contacts of particles on bed

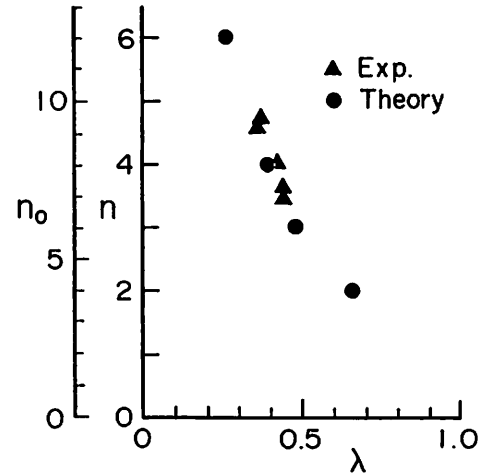


Fig. 17 Relation between the number of contacts on a particle in random packing or the number of neighbour particles of a particle on bed and porosity (Ref.(11))

Equilibrium Concentration Distribution of Suspended Load

Concentration distribution of suspended load can be calculated from $f(\hat{z}_p, \hat{T})$ and \hat{q}_{su} . In this procedure the discussion concerning the reference level and concentration at the level is not needed at all. Concentration distribution of suspended load is expressed in the equilibrium condition as

$$C(\hat{z}) = \int_0^\infty \hat{q}_{su} f(\hat{z}, \hat{t}) d\hat{t} \quad (38)$$

Eq.(38) is solved from Eqs.(30) and (37). In Fig. 18 the result of Eq.(38) and experimental results by Ashida and Michiue (1) under the condition of $d = 0.009$ cm, $u_* = 4.02$ cm/sec, $\sigma/\rho = 2.65$, $h = 7.05$ cm, $U = 63.8$ cm/sec, $ck^2 = 1.8$ and $\eta_s = 0.33$ are shown. In this figure the Rouse's distribution is also plotted. It is not apparent which distribution is more consistent with the experimental results. But this model is excellent in the points that there is no need to give uncertain reference level and the concentration at the reference level.

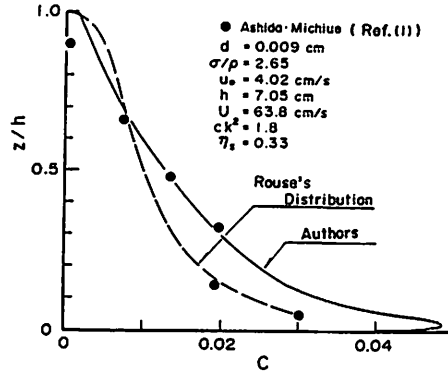


Fig. 18 Equilibrium concentration profile of suspended load

APPLICATION FOR NON-EQUILIBRIUM SUSPENDED LOAD WITH ARMOURING PROCESS

Non-equilibrium Suspended Load

Assumed that bed configuration is as follows: Upstream from the section at $X = 0$ is an unmovable bed and downstream from that section is a movable bed which consists of nonuniform sediments. If the gravels with the maximum diameter on the bed cannot be moved, the bed slope does not change too much and an armour coat is formed. Under this condition the so called parallel degradation must be occurred, and suspended load varies with space and time.

Suspended load of particle i with diameter d_i is evaluated under above condition by following manner. If the particle i entrained from the bed at $x = x_0$ and $t = t_0$ is moving at $x = X$ and $t = T$, concentration distribution of particle i at $x = X$ and $t = T$ is written as

$$C_i(X, z, T) = \int_0^{\tau_{\max i}} (1/\sigma) q_{sui}(x_0, t_0) f_i(x_0, z, \tau, t_0) d\tau \quad (39)$$

where $\tau = T - t_0$; $X = x_0 + \bar{u}_{pi}(\tau)\tau$; $\tau_{\max i} = \min(T, X/\bar{u}_{pi}(\tau_{\max i}))$; $q_{sui}(x_0, t_0)$ = the pick up rate of particle i at $x = x_0$ and $t = t_0$; $f(x_0, z, \tau, t_0)$ = the p.d.f. of vertical elevation of the particle i after τ since it is entrained at $x = x_0$ and $t = t_0$; $\bar{u}_{pi}(\tau)$ = the mean streamwise velocity of particle i from $t = t_0$ to $t = t_0 + \tau$.

Assuming that $\bar{u}_{pi}(\tau)$ is $\bar{u}_p = k_u U$, Eq.(39) is transformed into

$$C_i(X, z, T) = \int_{X_{\min}}^X (1/\sigma) q_{sui}(x_0, T - \frac{X-x_0}{\bar{u}_p}) f_i(x_0, z, \frac{X-x_0}{\bar{u}_p}, T - \frac{X-x_0}{\bar{u}_p}) / \bar{u}_p dx_0 \quad (40)$$

where $X_{\min} = \max(0, X - \bar{u}_p T)$ and k_u is a constant coefficient.

Hence suspended load of particle i at $x = X$ and $t = T$ is expressed as

$$q_{si}(X, T) = \int_0^h C_i(X, z, T) \bar{u}_p dz \quad (41)$$

Moreover, the probability in which a particle i would be suspended after τ from entrainment is written as

$$p_{si}(x_0, \tau, t_0) = \int_0^h f_i(x_0, z, \tau, t_0) dz \quad (42)$$

Equation (41) is transformed from Eqs.(39) and (42) into

$$q_{si}(X, T) = \int_{x_{\min}}^X (1/\sigma) q_{sui}(x_0, T - \frac{X-x_0}{\bar{u}_p}) p_{si}(x_0, \frac{X-x_0}{\bar{u}_p}, T - \frac{X-x_0}{\bar{u}_p}) dx_0 \quad (43)$$

Equation (43) can be solved with Eqs.(30) and (37).

A Model of the Armouring Process in Consideration of Suspended Load

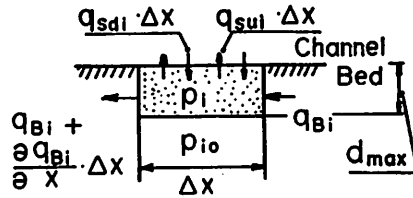


Fig. 19 A model for exchange of bed materials

In the armouring process the depth of the mixing layer is considered to be the maximum diameter d_{\max} of bed materials. The model of mixing of the transported sediment and the bed materials can be considered as shown in Fig. 19. If the porosity of the bed materials is constant, the continuity equation of sediment and grain size distribution are written as

$$\frac{\partial z}{\partial t} + \frac{1}{1-\lambda} \frac{\partial q_B}{\partial x} + \frac{q_{su} - q_{sd}}{1-\lambda} = 0 \quad (44)$$

$$\frac{\partial p_i}{\partial t} = \frac{1}{d_{\max}} \left\{ -\frac{1}{1-\lambda} \frac{\partial q_{Bi}}{\partial x} - \frac{1}{1-\lambda} (q_{sui} - q_{sdi}) - \frac{\partial z}{\partial t} p_{oi} \right\} \quad (45)$$

where $q_B = \sum q_{Bi}$; $q_{su} = \sum q_{sui}$; $q_{sd} = \sum q_{sdi}$; q_{Bi} , q_{sui} and q_{sdi} = bed load, pick up rate and deposition rate of particle i , respectively; p_i and p_{oi} = the rate of particle i in the mixing layer and the layer lower than the mixing layer respectively; and λ = porosity.

Bed load is calculated from Ashida and Michiue formulas (3) as

$$\frac{q_{Bi}}{p_i u_{*i} d_i} = 17 \tau_{*i} (1 - \tau_{*ci} / \tau_{*i}) (1 - \sqrt{\tau_{*ci} / \tau_{*i}}) \quad (46)$$

where d_i is the mean diameter of particle i , τ_{*i} is non-dimensional tractive force for d_i , τ_{*ci} is non-dimensional critical tractive force for d_i . τ_{*ci} is calculated from Egiazaroff's equation and it's modified equation by Ashida and Michiue (3) as

$$\frac{\tau_{*ci}}{\tau_{*cm}} = \left\{ \frac{\log_{10} 19}{\log_{10}(19d_i/d_m)} \right\}^2 \quad (d_i/d_m \geq 0.4) \quad (47-a)$$

$$\frac{\tau_{*ci}}{\tau_{*cm}} = 0.85 (d_m/d_i) \quad (d_i/d_m < 0.4) \quad (47-b)$$

where d_m = the mean diameter on the bed surface ;and τ_{*cm} = nondimensional critical tractive force for d_m .

Assuming that p_f equals approximately p_i , q_{sui} is calculated from

$$q_{sui}(x_0, t_0)/\rho\sqrt{gd_i} = \frac{2}{3} K p_i \sqrt{6(s+1)/\pi} \int_{\eta_{0i}}^{\infty} (u_*/\sqrt{gd_i}) \sqrt{ck_i^2 \eta - (\pi/8) C_{D0i} \xi_{0i}^2} \frac{1}{\sqrt{2\pi}} \exp(-\frac{1}{2} \eta^2) d\eta \quad (48)$$

where $\eta_{0i} = (\pi/8) C_{D0i} \xi_{0i}^2 / (ck_i^2)$; $C_{D0i} = 2 + 24\nu/(w_{0i}d_i)$; $\xi_{0i} = w_{0i}/u_*$; w_{0i} = the fall velocity of particle i ; and k_i is the coefficient of the shelter effect for particle i .

q_{sdi} is derived from eq.(48) and $p_{si}(x_0, \tau, t_0)$ as

$$q_{sdi}(X, T) = \int_{x_{min}}^X (1/\sigma) q_{sui}(x_0, T - \frac{X-x_0}{\bar{u}_p}) \frac{d}{dx} p_{si}(x, \frac{X-x_0}{\bar{u}_p}, T - \frac{X-x_0}{\bar{u}_p}) dx_0 \quad (49)$$

It is very complicated to calculate $p_{si}(x_0, \tau, t_0)$ from the present model. But if the diameter of a particle is small, the vertical velocity of a particle approaches $w_f - w_0$ rapidly when the upward flow velocity, w_f , acts on the particle. So the following approximated method will be proposed for the analyzing of vertical particle motion. Particle motion is divided by mean duration of turbulent flow. Vertical particle velocity is approximated to $w_f - w_0$ in each step. If a particle is transported to $z_p = z_{pn+1}$ from $z_p = z_{pn}$ vertically in step $n+1$, the p.d.f. of z_{pn+1} under the condition of z_{pn} is expressed as

$$g_i(z_{pn+1} | z_{pn}) = \frac{1}{\sqrt{2\pi} u_* t_{em}} \exp \left\{ -\frac{1}{2} \left(\frac{z_{pn+1} - z_{pn} + w_0 t_{em}}{u_* t_{em}} \right)^2 \right\} \quad (50)$$

Particle elevation at the end of step 1 is given by mean value of Eq.(10-b). So the p.d.f. of elevation of particle i at the end of step n is given by

$$f_{ni}(z_{pn}) = \int_0^h f_{n-1i}(z_{pn-1}) g_i(z_{pn} | z_{pn-1}) dz_{pn-1} \quad (51-a)$$

$$f_{1i}(z_{p1}) = \delta(z_{p1} - \bar{z}_{p1}) \quad (51-b)$$

where \bar{z}_{p1} = the mean value of Eq.(10-b).

This method is almost similar to Yalin, M.S. and B.M. Krishnappan's (13). But the way to calculate z_{p1} , which is the most important point, is due to the mechanism of suspension in this model. The probability of continuing to be

suspended till the end of step n is $p_{sni} = \int_0^h f_{ni}(z_{pn}) dz_{pn}$, and if a suspended particle at $x = x_0$ and $t = t_0$ is situated in the process of step n , $p_{si}(x_0, \tau, t_0)$ is expressed as

$$p_{si}(x_0, \tau, t_0) = \frac{(\tau - T_{n-1})p_{sn-1i} + (T_n - \tau)p_{sni}}{t_{em}} \quad (52)$$

where T_i = terminate time of step i .

Though f_{ni} varies with armouring, f_{ni} can be assumed to be constant because hydraulic conditions do not change too much in parallel degradation and the effect of bed conditions on particle motion is less if a particle is entrained into the flow from the bed. In Fig. 20 the comparison between the approximated method and Eq.(42) under the experimental condition mentioned in the next section is shown. This figure indicates that the approximated method allows the calculation of p_{si} .

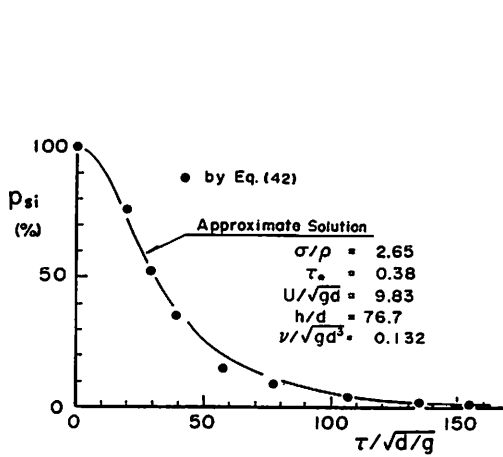


Fig. 20 Comparison between p_{si} calculated by eq.(42) and ones by its approximate method

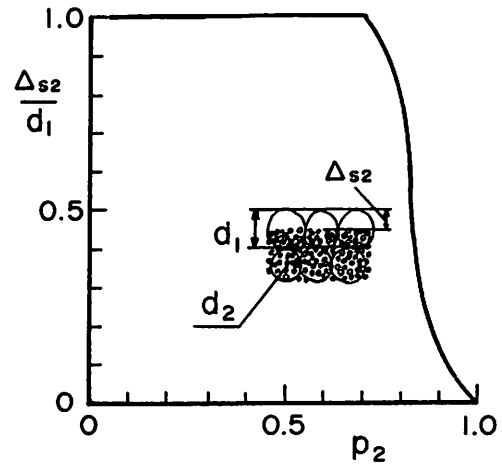


Fig. 21 Relation between percentage of sand on bed and the position of it among gravels

It is necessary to relate the mean diameter of bed materials, d_m , and non-dimensional level of particle i on a bed, Δ_{si}/d_r , to p_i in order to obtain coefficient of lift force and shelter effect. From Fig. 9 c is obtained for $d_m u_* / \nu$, where d_m is calculated from p_i . Otherwise, it is generally difficult to gain the relation between Δ_{si}/d_r and p_i . Two size mixed materials such as gravel ($i=1$) and sand ($i=2$), is considered as the simple case. Δ_{s2} is obtained from the ratio of volume of gravel and sand within d_1 from bed surface, which is calculated from p_1 and p_2 . The relation between Δ_{s2}/d_1 and p_2 is shown in Fig. 21. As d_r is d_1 , k_2 is gained from Fig. 10. This method may be applicable for general non-uniform materials. A coefficient of the shelter effect k_i for particle i can be obtained by dividing the materials into two classes, one of which is the materials of $d > d_i$, the other is the materials of $d < d_i$. The level Δ_{s2i} of the materials of $d < d_{1i}$ is obtained as in the two size mixed material case. As Δ_{si} is assumed to be Δ_{s2i} and d_r is assumed to be the mean diameter of materials of $d > d_i$, k_i is obtained from Fig. 10. But this method must be verified experimentally.

Thus, under the condition of quasi-uniform flow and the logarithmic law for resistance law, the variation of sediment discharge, bed elevation and mixing rate of bed materials with time and space can be analyzed.

Comparison Between Theoretical Results and Experimental Results

The experiment was performed with 0.3 m long and 8 m wide flume, and bed slope was 0.008. The grain size distribution of used sands M is shown in Fig. 22, which consisted of sand 1 and sand 2 with a mean diameter of 2.66 mm and 0.18 mm respectively. The area covered by the mixed materials was between 0.5 m and 6 m downstream section. Water discharge was $57 \text{ cm}^2/\text{sec}$ and initial shear velocity was 3.3 cm/sec . Bed elevation, water elevation, suspended load and mixing rate of bed materials were measured. Critical shear velocity for sand 1 is 4.56 cm/sec , and sand 2 only was transported as bed load and suspended load.

In Fig. 23 the variation of p_1 and q_{s2} at $x = 5.5 \text{ m}$ with time is shown. This figure indicates that armour coat develops fully in the downstream area in about 10 minutes. In Fig. 24 the streamwise distribution of q_{s2} is shown. The region of equilibrium suspended load is not apparent even under initial conditions because of less measurement points and transportation of bed materials at initial time. But this figure indicates that the region of non-equilibrium suspended load rapidly spread in the downstream direction.

The armouring process in this experiment was simulated by this model under the conditions of $\Delta x = 5 \text{ cm}$, $\Delta t = \Delta x/u_p$, $k_s/d_m = 2$, $z_{ps}/h = 0.25$ and $k_u = 1.0$, where Δx = longitudinal place step; and Δt = time step. In Figs. 22 and 23 the theoretical results are also shown. These figures indicate that theoretical results of non-equilibrium suspended load favorably account for the experimental results. Hence, the present model will be sufficiently applicable to analyse non-equilibrium suspended load situations.

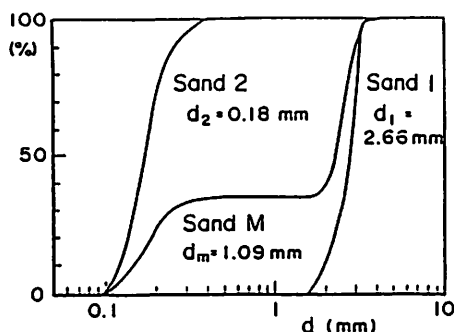


Fig. 22 Grain size distribution of the sands used in the experiment

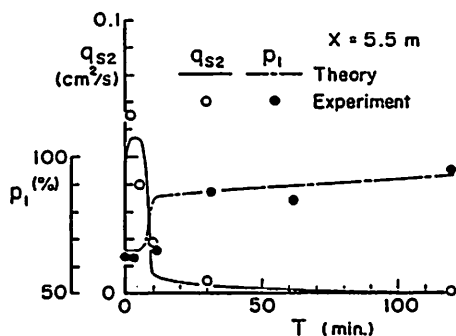


Fig. 23 Comparison between theoretical results and experimental ones concerning percentage of gravel on bed and suspended load of sand at $X = 5.5 \text{ m}$

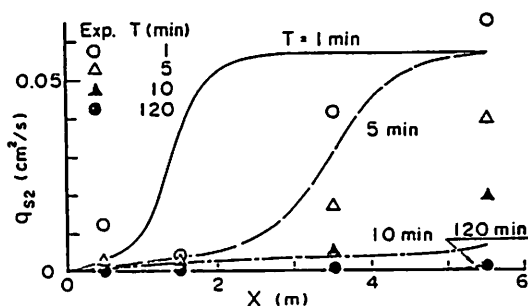


Fig. 24 Comparison between theoretical results and experimental ones concerning variation of suspended load with longitudinal distance

CONCLUSIONS

The mechanism of particle suspension was investigated theoretically on the simultaneous observation of particle motion and turbulent structure by using a high speed video camera and visualization technique. Pick up rate and a stochastic model for motion of a suspended particle were formulated, and a method to calculate suspended load both under equilibrium and non-equilibrium conditions was proposed. The main results are summarized as follows:

(1) A particle on a rough bed is entrained into the flow by lift force due to an accelerated upward flow which occurs during an ejection event of bursting. Though the lift force decreases to about zero in a short period after the entrainment, the particle further rises up by drag force due to the same upward flow. Then, the particle rises up or settles down corresponding to upward or downward turbulent flows.

(2) The vertical dynamic forces acting on the particle were evaluated by the equation of particle motion and locus of particle motion obtained by the experiment.

(3) A stochastic model for analyzing the suspended particle motion was proposed. It was verified that the model was applicable to simulating the characteristics of motion of suspended particle, for example the vertical dispersion process and step length.

(4) A method to calculate pick up rate was formulated in the consideration of the shelter effect due to gravels so that it was able to apply for nonuniform sediment. It was shown that the present method was applicable to calculation of pick up rate of uniform sediments and nonuniform ones.

(5) By using the formula for pick up rate and stochastic model proposed in this paper, a method to calculate suspended load both in equilibrium and in non-equilibrium conditions was proposed. Non-equilibrium suspended load with armouring process was calculated using the present method. This results sufficiently agreed with experimental results.

REFERENCES

1. Ashida, K and M. Michiue : Laboratory study of suspended load discharge in alluvial channels, *Annals, D.P.R.I.*, No.10B, pp.63-79, 1967 (in Japanese).
2. Ashida, K and M. Michiue : Study on the suspended sediment (1), *Annals, D.P.R.I.*, No.13B, pp.233-242, 1970 (in Japanese).
3. Ashida, K and M. Michiue : Study on hydraulic resistance and bed-load transport rate in alluvial streams, *Proc. JSCE*, pp.59-69, 1972 (in Japanese).
4. Ashida, K and M. Fujita : Threshold condition of particle suspension, *Proc. 27th Conference on hydraulics, JSCE*, pp.311-316, 1983 (in Japanese).
5. Einstein, H.A. : The bed load function for sediment transportation in open channel flow, *USDA, Soil Conservation Service, Technical Bulletin*, No.1026, pp.1-71, 1950.
6. Grass, A.J. : Structural features of turbulent flow over smooth and rough boundaries, *J.F.M.*, Vol.50, pp.233-255, 1971.
7. Hinze, J.O. : *Turbulence*, McGraw-Hill, pp.353-354, 1959.
8. Itakura, T and T. Kishi : Open channel flow with suspended sediments, *Proc. ASCE, Journal of the hydraulics division*, HY8, pp.1325-1342, 1980.
9. Jackson, R.G. : Sedimentological and fluid dynamic implications of the turbulent bursting phenomenon in geophysical flows, *J.F.M.*, pp.531-560, 1976.
10. Nezu, I and H. Nakagawa : Bursting phenomenon in a turbulent shear flow and its physical model, *Proc. 22th Conference on Hydraulics, JSCE*, pp.29-36, 1978 (in Japanese).
11. Smith, W.O., P.D. Foote and P.F. Busang : *Phys. Rev.*, 34, 1929.
12. Sumer, B.M. and R. Deigaard : Experimental investigation of motions of suspended heavy particles and the bursting process, *Technical University of Denmark, Series Paper*, No.23, 1979.
13. Yalin, M.S. and B.M. Krishnappan : A probabilistic method for determining the distribution of suspended solids in open channels, *I.A.H.R., International symposium on river mechanics*, A52-1-A52-12, 1973.

APPENDIX - NOTATION

The following symbols are used in this paper:

a	= constant on relation between w_{fe} and T_{e1} ;
A	= $3/(2s+3)$;
B	= $36 \hat{v}/(2s+3)$;
c	= coefficient of lift force;
c_1	= experimental constant;
c_2	= constant (ratio of w_{fe} or w_{fee} to u_*);
c_3	= ratio of T_{e1} to T_{ee} ;
C	= $-2s/(2s+3)$;
C_D	= coefficient of drag force;
C_{D0}	= C_D for $w_p = w_0$;
C_{D0i}	= C_{D0} of particle i ;
d	= particle diameter;
d_{1i}	= mean diameter of particles larger than particle with a diameter of d_i among bed materials;
d_m	= mean diameter of bed particles;
d_{max}	= maximum diameter of bed materials;
d_r	= mean diameter of representative roughness gravels;
$f(\hat{z}_p, \hat{T})$	= probability density function of level of suspended particle at $t = T$;
f_i	= probability density function of level of particle i ;
$f_{ni}(z_{pn})$	= probability density function of level of particle i at the end of step n ;
$f_{t_c}(t_c)$	= probability density function of t_c ;
$\hat{f}_{w_f}(\hat{w}_f)$	= probability density function of w_f ;
$\hat{f}_{w_{fe}}(\hat{w}_{fe})$	= probability density function of w_{fe} ;
$\hat{f}_{w_{p0}}(\hat{w}_{p0})$	= probability density function of w_{p0} ;
$\hat{f}_{F_{L0}}(\hat{F}_{L0})$	= probability density function of F_{L0} ;
F_D	= drag force;
F_i	= function;
F_L	= lift force;
F_{Li}	= lift force at $t = 0.01i$ sec;
$F_{L0'}$	= lift force with upward flow near the bed;
F_{L0}	= standard deviation of F_{L0} ;
g	= acceleration due to gravity;
$g_i(\hat{z}_p \hat{z}_{p1})$	= probability density function of level of suspended particle at the end of step i under the case that z_p equals z_{p1} at the end of step 1 ;

G	= submerged grain weight;
G_i	= function;
h	= flow depth;
$h(\hat{z}_p, \hat{T} \hat{z}_{p1})$	= probabilistic density function of level at $t = T$ under the condition of $z_p = z_{p1}$ at the end of step 1;
I	= energy slope;
k	= coefficient of shelter effect by gravels;
k_1	= rate of particles able to be picked up to all the particles on the bed surface;
k_2	= constant (rate of t_c to t_*);
k_i	= coefficient of shelter effect on particle i by gravels;
k_s	= equivalent sand roughness;
k_u	= constant;
K	= k_1/k_2 ;
n	= number of neighbour particles lying around a particle on the bed surface;
n_0	= number of particles contacting a particle in the random packing;
N_B	= number of particles per unit area;
P_f	= rate of particle with a diameter of d within the materials on the bed surface;
p_i	= rate of particle i in the mixing layer;
p_{i0}	= rate of particle i in the layer lower than the mixing layer;
p_{si}	= probability in which a particle entrained from a bed continues to be suspended;
p_{sni}	= p_{si} at the end of step i ;
q_B	= bed load;
q_{Bi}	= bed load of particle i ;
q_{si}	= suspended load of particle i ;
q_{sd}	= deposition rate;
q_{sdi}	= deposition rate of particle i ;
q_{su}	= pick up rate of suspended particle;
q_{sui}	= q_{su} of particle i ;
R_*	= grain size Reynolds number;
s	= $\sigma/\rho - 1$
t	= time;
t_c	= exchange time;
t_e	= duration of upward flow mass;
t_{em}	= Lagrangean mean duration of turbulence;
t_s	= duration of suspension of particle;
t_*	= duration of F_{L0} ;

T_{ee}	= Eulerian duration of upward flow at a level;
T_{el}	= Lagrangean duration of upward flow near the bed;
T_n	= terminal time of step n ;
T_u	= period of occurrence of bursting;
u_f	= streamwise flow velocity;
u_p	= streamwise particle velocity;
$u_p(T)$	= mean streamwise velocity of particle from $t = 0$ to $t = T$;
$u_{pi}(T)$	= $u_p(T)$ of particle i ;
u_*	= shear velocity;
U	= mean streamwise flow velocity;
U_{max}	= maximum streamwise flow velocity;
w_f	= vertical turbulent velocity;
w_f'	= vertical turbulence intensity;
w_{fe}	= vertical velocity of upward flow mass near the bed;
w_{fee}	= vertical velocity of fluid at a level;
w_0	= fall velocity of particle;
w_{0i}	= fall velocity of particle i ;
w_p	= vertical velocity of particle;
w_{pi}	= w_p in step i ;
w_{p0}	= initial value of w_p in calculation of particle motions;
X_e	= distance in which suspended load increases to equilibrium value from zero;
X_p	= step length of suspended particle;
X_{Lm}	= mean step length of suspended particle;
X_{min}	= $\max(0, X - \bar{u}_p T)$;
z_L	= mean level of upward flow mass near the bed;
z_p	= level of particle;
z_{pi}	= z_p in step i ;
z_{pm}	= time average level of particle which continues to be suspended during time T ;
z_{p0}	= initial value of z_p in calculation of particle motions;
z_{ps}	= mean level of suspended particle;
z_{pmT}	= mean level of suspended particle at $t = T$;
α	= constant;
Δ	= thickness within which lift force keep positive near a bed;
Δt	= time step;
Δ_s	= distance between particle surface and the top of the representative roughness;
Δx	= longitudinal place step;
η	= F_{L0}/F_{L0}' ;

η_0	$= (\pi/8)C_{D0}\rho\xi_0^2/(ck^2);$
$\eta(\hat{z}_p, \hat{t} \hat{w}_{pi}, \hat{z}_{pi})$	$=$ probability density function of \hat{z}_p where a suspended particle stays after \hat{t} ;
η_s	$= z_{ps}/h;$
κ	$=$ von Kármán's constant;
λ	$=$ porosity;
ν	$=$ kinematic viscosity;
ξ_0	$= w_0/u_*;$
$\xi(\hat{z}_{p1})$	$=$ probabilistic density function of $\hat{z}_{p1};$
ρ	$=$ density of fluid;
σ	$=$ density of particle;
τ	$=$ time;
τ_*	$=$ non-dimensional tractive force;
τ_{*c}	$=$ non-dimensional critical tractive force on bed load;
τ_{*i}	$=$ non-dimensional tractive force for d_i ;
τ_{*s}	$=$ non-dimensional critical tractive force on suspended load;
τ_{*ci}	$= \tau_{*c}$ for d_i ;
τ_{*cm}	$= \tau_{*c}$ for d_m ;